

Measurement of B_s^0 and D_s^- Meson Lifetimes

R. Aaij *et al.**

(LHCb Collaboration)

(Received 10 May 2017; published 8 September 2017)

We report on a measurement of the flavor-specific B_s^0 lifetime and of the D_s^- lifetime using proton-proton collisions at center-of-mass energies of 7 and 8 TeV, collected by the LHCb experiment and corresponding to 3.0 fb^{-1} of integrated luminosity. Approximately 407 000 $B_s^0 \rightarrow D_s^{(*)-} \mu^+ \nu_\mu$ decays are partially reconstructed in the $K^+ K^- \pi^- \mu^+$ final state. The B_s^0 and D_s^- natural widths are determined using, as a reference, kinematically similar $B^0 \rightarrow D^{(*)-} \mu^+ \nu_\mu$ decays reconstructed in the same final state. The resulting differences between widths of B_s^0 and B^0 mesons and of D_s^- and D^- mesons are $\Delta_\Gamma(B) = -0.0115 \pm 0.0053(\text{stat}) \pm 0.0041(\text{syst}) \text{ ps}^{-1}$ and $\Delta_\Gamma(D) = 1.0131 \pm 0.0117(\text{stat}) \pm 0.0065(\text{syst}) \text{ ps}^{-1}$, respectively. Combined with the known B^0 and D^- lifetimes, these yield the flavor-specific B_s^0 lifetime, $\tau_{B_s^0}^{\text{fs}} = 1.547 \pm 0.013(\text{stat}) \pm 0.010(\text{syst}) \pm 0.004(\tau_B) \text{ ps}$ and the D_s^- lifetime, $\tau_{D_s^-} = 0.5064 \pm 0.0030(\text{stat}) \pm 0.0017(\text{syst}) \pm 0.0017(\tau_D) \text{ ps}$. The last uncertainties originate from the limited knowledge of the B^0 and D^- lifetimes. The results improve upon current determinations.

DOI: 10.1103/PhysRevLett.119.101801

Comparisons of precise measurements and predictions associated with quark-flavor dynamics probe the existence of unknown particles at energies much higher than those directly accessible at particle colliders. The precision of the predictions is often limited by the strong-interaction theory at low energies, where calculations are intractable. Predictive power is recovered by resorting to effective models such as heavy-quark expansion [1] which rely on an expansion of the quantum chromodynamics corrections in powers of $1/m$, where m is the mass of the heavy quark in a bound system of a heavy quark and a light quark. These predictions are validated and refined using lifetime measurements of heavy hadrons. Hence, improved lifetime measurements ultimately enhance the reach in searches for nonstandard-model physics. Currently, more precise measurements are particularly important as predictions of the lifetime ratio between B_s^0 and B^0 mesons show a 2.5 standard-deviation discrepancy from measurements.

Measurements of the “flavor-specific” B_s^0 meson lifetime, $\tau_{B_s^0}^{\text{fs}}$, have additional relevance. This empirical quantity is a function of the natural widths of the two mass eigenstates resulting from $B_s^0 - \bar{B}_s^0$ oscillations, and therefore allows an indirect determination of the width difference that can be compared with direct determinations in tests for nonstandard-model physics [2]. The lifetime $\tau_{B_s^0}^{\text{fs}}$ is

measured with a single-exponential fit to the distribution of decay time in final states to which only one of B_s^0 and \bar{B}_s^0 mesons can decay [3]. The current best determination, $\tau_{B_s^0}^{\text{fs}} = 1.535 \pm 0.015(\text{stat}) \pm 0.014(\text{syst}) \text{ ps}$ [4], obtained by the LHCb Collaboration using hadronic $B_s^0 \rightarrow D_s^- \pi^+$ decays, has similar statistical and systematic uncertainties. Semileptonic B_s^0 decays, owing to larger signal yields than in hadronic decays, offer richer potential for precise $\tau_{B_s^0}^{\text{fs}}$ measurements. However, neutrinos and low-momentum neutral final-state particles prevent the full reconstruction of such decays. This introduces systematic limitations associated with poor knowledge of backgrounds and difficulties in obtaining the decay time from the observed decay-length distribution. Indeed, the result $\tau_{B_s^0}^{\text{fs}} = 1.479 \pm 0.010(\text{stat}) \pm 0.021(\text{syst}) \text{ ps}$ [5], based on a $B_s^0 \rightarrow D_s^{(*)-} \mu^+ \nu_\mu X$ sample from the D0 Collaboration, is limited by the systematic uncertainty. Throughout this Letter, the symbol X identifies any decay product, other than neutrinos, not included in the candidate reconstruction, and the inclusion of charge-conjugate processes is implied.

In this Letter, we use a novel approach that suppresses the above limitations and achieves a precise measurement of the flavor-specific B_s^0 meson lifetime. The lifetime is determined from the variation in the B_s^0 signal yield as a function of decay time, relative to that of B^0 decays that are reconstructed in the same final state and whose lifetime is precisely known. The use of kinematically similar B^0 decays as a reference allows the reduction of the uncertainties from partial reconstruction and lifetime-biasing selection criteria. The analysis also yields a significantly improved determination of the D_s^- lifetime over the current

*Full author list given at the end of the article.

Published by the American Physical Society under the terms of the Creative Commons Attribution 4.0 International license. Further distribution of this work must maintain attribution to the author(s) and the published article's title, journal citation, and DOI.

best result, $\tau_{D_s^-} = 0.5074 \pm 0.0055(\text{stat}) \pm 0.0051(\text{syst})$ ps, reported by the FOCUS Collaboration [6].

We analyze proton-proton collisions at center-of-mass energies of 7 and 8 TeV collected by the LHCb experiment in 2011 and 2012 and corresponding to an integrated luminosity of 3.0 fb^{-1} . We use a sample of approximately 407 000 $B_s^0 \rightarrow D_s^{*-}\mu^+\nu_\mu$ and $B_s^0 \rightarrow D_s^-\mu^+\nu_\mu$ “signal” decays, and a sample of approximately 108 000 $B^0 \rightarrow D^{*-}\mu^+\nu_\mu$ and $B^0 \rightarrow D^-\mu^+\nu_\mu$ “reference” decays. The D candidates are reconstructed as combinations of K^+ , K^- , and π^- candidates originating from a common vertex, displaced from any proton-proton interaction vertex. The $B_{(s)}^0$ candidates, $K^+K^-\pi^-\mu^+$, are formed by D candidates associated with muon candidates originating from another common displaced vertex. We collectively refer to the signal and reference decays as $B_s^0 \rightarrow [K^+K^-\pi^-]_{D_s^{(*)-}}\mu^+\nu_\mu$ and $B^0 \rightarrow [K^+K^-\pi^-]_{D^{(*)-}}\mu^+\nu_\mu$, respectively. A fit to the ratio of event yields between the signal and reference decays as a function of $B_{(s)}^0$ decay time, t , determines $\Delta_\Gamma(B) \equiv 1/\tau_{B_s^0}^{\text{fs}} - \Gamma_d$, where Γ_d is the known natural width of the B^0 meson. A similar fit performed as a function of the $D_{(s)}^-$ decay time determines the decay-width difference between D_s^- and D^- mesons, $\Delta_\Gamma(D)$. Event yields are determined by fitting the “corrected-mass” distribution of the candidates, $m_{\text{corr}} = p_{\perp,D\mu} + \sqrt{m_{D\mu}^2 + p_{\perp,D\mu}^2}$ [7]. This is determined from the invariant mass of the $D_{(s)}^-\mu^+$ pair, $m_{D\mu}$, and the component of its momentum perpendicular to the $B_{(s)}^0$ flight direction, $p_{\perp,D\mu}$, to compensate for the average momentum of unreconstructed decay products. The flight direction is the line connecting the $B_{(s)}^0$ production and decay vertices; the decay time $t = m_B Lk / p_{D\mu}$ uses the known $B_{(s)}^0$ mass, m_B [8], the measured $B_{(s)}^0$ decay length, L , and the momentum of the $D_{(s)}^-\mu^+$ pair, $p_{D\mu}$. The scale factor k corrects $p_{D\mu}$ for the average momentum fraction carried by decay products excluded from the reconstruction [9,10]. The effects of decay-time acceptances and resolutions, determined from simulation, are included.

The LHCb detector is a single-arm forward spectrometer equipped with precise charged-particle vertexing and tracking detectors, hadron-identification detectors, calorimeters, and muon detectors, optimized for the study of bottom- and charm-hadron decays [11,12]. Simulation [13,14] is used to identify all relevant sources of bottom-hadron decays, model the mass distributions, and correct for the effects of incomplete kinematic reconstructions, relative decay-time acceptances, and decay-time resolutions. The unknown details of the B_s^0 decay dynamics are modeled in the simulation through empirical form-factor parameters [15], assuming values inspired by the

known B^0 form factors [2]. We assess the impact of these assumptions on the systematic uncertainties.

The online selection requires a muon candidate, with transverse momentum exceeding 1.5–1.8 GeV/ c , associated with one, two, or three charged particles, all with origins displaced from the proton-proton interaction points [16]. In the offline reconstruction, the muon is combined with charged particles consistent with the topology and kinematics of signal $B_s^0 \rightarrow [K^+K^-\pi^-]_{D_s^{(*)-}}\mu^+\nu_\mu$ and reference $B^0 \rightarrow [K^+K^-\pi^-]_{D^{(*)-}}\mu^+\nu_\mu$ decays. The range of $K^+K^-\pi^-$ mass is restricted around the known values of the $D_{(s)}^-$ meson masses such that cross-contamination between signal and reference samples is smaller than 0.1%, as estimated from simulation. We also reconstruct “same-sign” $K^+K^-\pi^-\mu^-$ candidates, formed by charm and muon candidates with same-sign charge, to model combinatorial background from accidental $D_{(s)}^-\mu^+$ associations. The event selection is optimized toward suppressing the background under the charm signals and making same-sign candidates a reliable model for the combinatorial background: track- and vertex-quality, vertex-displacement, transverse-momentum, and particle-identification criteria are chosen to minimize shape and yield differences between same-sign and signal candidates in the $m_{D\mu} > 5.5 \text{ GeV}/c^2$ region, where genuine bottom-hadron decays are kinematically excluded and combinatorial background dominates. Mass vetoes suppress background from misreconstructed decays such as $B_s^0 \rightarrow \psi^{(\prime)}(\rightarrow \mu^+\mu^-)\phi(\rightarrow K^+K^-)$ decays where a muon is misidentified as a pion, $\Lambda_b^0 \rightarrow \Lambda_c^+(\rightarrow pK^-\pi^+)\mu^-\bar{\nu}_\mu X$ decays where the proton is misidentified as a kaon or a pion, and $B_{(s)}^0 \rightarrow D_{(s)}^-\pi^+$ decays where the pion is misidentified as a muon. Significant contributions arise from decays of a bottom hadron into pairs of charm hadrons, one peaking at the $D_{(s)}^-$ mass and the other decaying semileptonically, or into single charm hadrons and other particles. Such decays include $B_{(s)}^0 \rightarrow D_{(s)}^{(*)-}D_{(s)}^+$, $B^+ \rightarrow \bar{D}^{(*)0}D^{(*)+}$, $B^+ \rightarrow D^-\mu^+\nu_\mu X$, $B^+ \rightarrow D_s^{(*)-}K^+\mu^+\nu_\mu X$, $B^0 \rightarrow D_s^{(*)-}K^0\mu^+\nu_\mu X$, $B_s^0 \rightarrow D^0D_s^-K^+$, $B_s^0 \rightarrow D^-D_s^+K^0$, $\Lambda_b^0 \rightarrow \Lambda_c^+D_s^{(*)-}X$, and $\Lambda_b^0 \rightarrow D_s^+\Lambda\mu^-\bar{\nu}_\mu X$ decays. We suppress these backgrounds with a threshold, linearly dependent on m_{corr} , applied to the $D_{(s)}^-$ momentum component perpendicular to the $B_{(s)}^0$ flight direction. Finally, a $t > 0.1$ ps requirement on the $D_{(s)}^-$ proper decay time renders the signal- and reference-decay acceptances as functions of decay time more similar, with little signal loss.

A total of approximately 468 000 (141 000) signal (reference) candidates, formed by combining $K^+K^-\pi^-$ candidates in the D_s^- (D^-) signal range with μ^+ candidates, satisfy the selection. Figure 1 shows the relevant mass distributions. The enhancements of the signal and reference distributions over the corresponding same-sign distributions for $m_{D\mu} < 5.5 \text{ GeV}/c^2$ are due to bottom-hadron

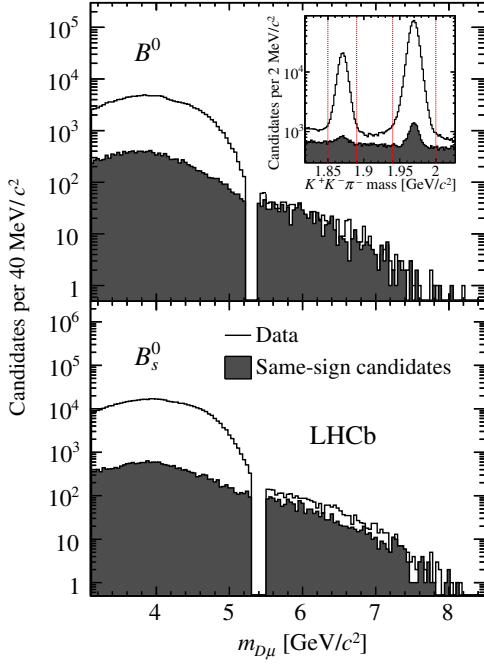


FIG. 1. Distributions of $D\mu$ mass for (top panel) reference candidates, formed by combining $D^- \rightarrow K^+K^-\pi^-$ candidates with μ^+ candidates, and (bottom panel) signal candidates formed by $D_s^- \rightarrow K^+K^-\pi^-$ candidates combined with μ^+ candidates. The inset shows the $K^+K^-\pi^-$ -mass distribution with vertical lines enclosing the D^- (D_s^-) candidates used to form the reference (signal) candidates. The dark-filled histograms show same-sign candidate distributions.

decays. The absence of candidates at $m_{D\mu} \approx 5.3 \text{ GeV}/c^2$ results from the $B_{(s)}^0 \rightarrow D_{(s)}^-\pi^+$ veto. The two peaks in the $K^+K^-\pi^-$ distributions of same-sign candidates are due to genuine charm decays accidentally combined with muon candidates. Along with $B_s^0 \rightarrow [K^+K^-\pi^-]_{D_s^{(*)-}}\mu^+\nu_\mu$ decays, many B_s^0 decays potentially useful for the lifetime measurement contribute signal candidates, including decays into $D_{(s)}^{**}(\rightarrow D_s^{(*)-}X)\mu^+\nu_\mu$, $D_s^-\tau^+(\rightarrow\mu^+\nu_\mu\bar{\nu}_\tau)\nu_\tau$, $D_s^{*-}(\rightarrow D_s^-X)\tau^+(\rightarrow\mu^+\nu_\mu\bar{\nu}_\tau)\nu_\tau$, and $D_s^{**}(\rightarrow D_s^{(*)-}X) \times \tau^+(\rightarrow\mu^+\nu_\mu\bar{\nu}_\tau)\nu_\tau$ final states [17]. Similarly, along with the $B^0 \rightarrow [K^+K^-\pi^-]_{D^{(*)-}}\mu^+\nu_\mu$ decays, potential reference candidates come from B^0 decays into $D^{**}(\rightarrow D^{(*)-}X)\mu^+\nu_\mu$, $D^-\tau^+(\rightarrow\mu^+\nu_\mu\bar{\nu}_\tau)\nu_\tau$, $D^{*-}(\rightarrow D^-X)\tau^+(\rightarrow\mu^+\nu_\mu\bar{\nu}_\tau)\nu_\tau$, and $D^{**}(\rightarrow D^{(*)-}X)\tau^+(\rightarrow\mu^+\nu_\mu\bar{\nu}_\tau)\nu_\tau$ final states. However, we restrict the signal (reference) decays solely to the $B_s^0 \rightarrow [K^+K^-\pi^-]_{D_s^{(*)-}}\mu^+\nu_\mu$ ($B^0 \rightarrow [K^+K^-\pi^-]_{D^{(*)-}}\mu^+\nu_\mu$) channels because they contribute 95% (91%) of the inclusive $K^+K^-\pi^-\mu^+$ yield from semileptonic B^0 (B_s^0) decays and require smaller and better-known k -factor corrections to relate the observed decay times to their true values.

A reliable understanding of the sample composition is essential for unbiased lifetime results. An unbiased

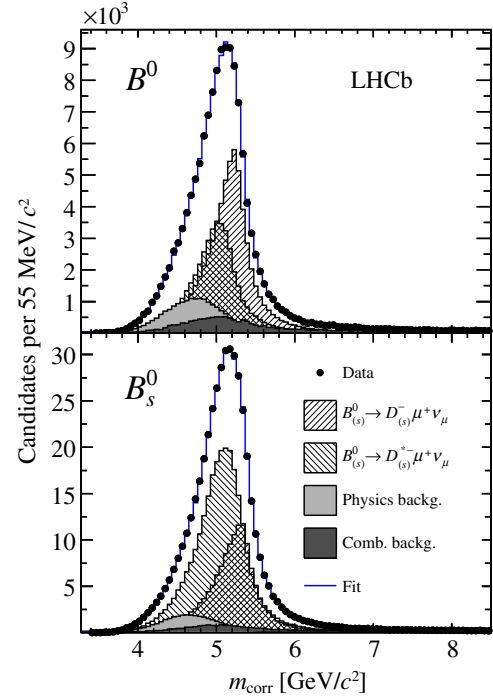


FIG. 2. Corrected-mass distributions for (top panel) reference $B^0 \rightarrow [K^+K^-\pi^-]_{D^{(*)-}}\mu^+\nu_\mu$ and (bottom panel) signal $B_s^0 \rightarrow [K^+K^-\pi^-]_{D_s^{(*)-}}\mu^+\nu_\mu$ candidates satisfying the selection. Results of the global composition-fit are overlaid. In the B_s^0 fit projection, the lower- and higher-mass background components described in the text are displayed as a single, merged “physics background” component.

determination from simulation of the acceptances and mass distributions as functions of decay time requires that the simulated sample mirrors the data composition. We therefore weight the composition of the simulated samples according to the results of a least-squares fit to the m_{corr} distributions in data, shown in Fig. 2. In the B_s^0 sample, such a global composition-fit includes the two signal components, $B_s^0 \rightarrow [K^+K^-\pi^-]_{D_s^{(*)-}}\mu^+\nu_\mu$ and $B_s^0 \rightarrow [K^+K^-\pi^-]_{D_s^{(*)-}}\mu^+\nu_\mu$, a combinatorial component, and two physics backgrounds. The physics backgrounds are formed by grouping together contributions with similar corrected-mass distributions, determined from simulation. They are divided into contributions at lower values of corrected mass [$B^0 \rightarrow D^{(*)-}D_s^{(*)+}$, $B^+ \rightarrow \bar{D}^{(*)0}D_s^{(*)+}$, and $D^{**}(\rightarrow D_s^{(*)-}X)\mu^+\nu_\mu$] and at higher corrected-mass values [$B^+ \rightarrow D_s^{(*)-}K^+\mu^+\nu_\mu X$, $B^0 \rightarrow D_s^{(*)-}K^0\mu^+\nu_\mu X$, and $B_s^0 \rightarrow D_s^-\tau^+(\rightarrow\mu^+\nu_\mu\bar{\nu}_\tau)\nu_\tau X$]. The distributions of all components are modeled empirically from simulation, except for the combinatorial component, which is modeled using same-sign data. Contributions expected to be smaller than 0.5% are neglected. The effect of this approximation and of possible variations of the relative proportions within each fit category are treated as contributions to the systematic

uncertainties. The fit p value is 62.1% and the fractions of each component are determined with absolute statistical uncertainties in the range 0.13%–0.91%. A simpler composition fit is used for the B^0 sample. Signal and combinatorial components are chosen similarly to the B_s^0 case; the contributions from $B^0 \rightarrow D^{*-}(\rightarrow D^{(*)-}X)\mu^+\nu_\mu$ and $B^+ \rightarrow D^-\mu^+\nu_\mu X$ decays have sufficiently similar distributions to be merged into a single physics-background component. The results of the corrected-mass fit of the reference sample also offer a validation of the approach, since the composition of this sample is known precisely from other experiments. The largest discrepancy observed among the individual fractional contributions is 1.3 statistical standard deviations.

The composition fit is sufficient for the determination of $\Delta_\Gamma(D)$, where no k -factor corrections are needed since the final state is fully reconstructed. We determine $\Delta_\Gamma(D)$ through a least-squares fit of the ratio of signal B_s^0 and reference B^0 yields as a function of the charm-meson decay time in the range 0.1–4.0 ps. The yields of signal $B_s^0 \rightarrow [K^+K^-\pi^-]_{D_s^{(*)-}\mu^+\nu_\mu}$ and reference $B^0 \rightarrow [K^+K^-\pi^-]_{D^{(*)-}\mu^+\nu_\mu}$ decays are determined in each of 20 decay-time bins with a m_{corr} fit similar to the global composition fit. The two signal and the two physics-background contributions are each merged into a single component according to the total proportions determined by the global fit and their decay-time dependence as determined from simulation. The fit includes the decay-time resolution and the ratio between signal and reference decay-time acceptances, which is determined from simulation to be uniform within 1%. The fit is shown in the top panel of Fig. 3; it has 34% p value and determines $\Delta_\Gamma(D) = 1.0131 \pm 0.0117 \text{ ps}^{-1}$.

The measurement of $\Delta_\Gamma(B)$ requires an acceptance correction for the differences between signal and reference decays and the k -factor correction. The acceptance correction accounts for the difference in decay-time-dependent efficiency due to the combined effect of the difference between D^- and D_s^- lifetimes and the online requirements on the spatial separation between D_s^- and B^0 decay vertices: we apply to the B_s^0 sample a per-candidate weight, $w_i \equiv \exp[\Delta_\Gamma(D)t(D_s^-)]$, based on the $\Delta_\Gamma(D)$ result and the D_s^- decay time, such that the D_s^- and D^- decay-time distributions become consistent. The k -factor correction is a candidate-specific correction, where the average missing momentum in a simulated sample is used to correct the reconstructed momentum in data. The k -factor dependence on the kinematic properties of each candidate is included through a dependence on $m_{D\mu}$, $k(m_{D\mu}) = \langle p_{D\mu}/p_{\text{true}} \rangle$, where p_{true} indicates the true momentum of the B^0 meson. The equalization of the compositions of simulated and experimental data samples ensures that the k -factor distribution specific to each of the four signal and reference decays is unbiased. We determine $\Delta_\Gamma(B)$ with the same fit

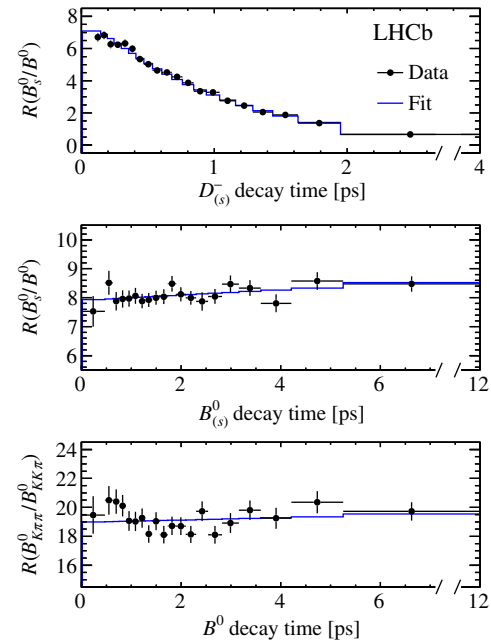


FIG. 3. Ratio between acceptance-corrected yields of signal $B_s^0 \rightarrow [K^+K^-\pi^-]_{D_s^{(*)-}\mu^+\nu_\mu}$ and reference $B^0 \rightarrow [K^+K^-\pi^-]_{D^{(*)-}\mu^+\nu_\mu}$ decay yields as a function of (top panel) charm-meson and (middle panel) bottom-meson decay time. The bottom panel shows the ratio between acceptance-corrected B^0 decay yields in the $[K^+\pi^-\pi^-]_{D^{(*)-}\mu^+\nu_\mu}$ and $[K^+K^-\pi^-]_{D^{(*)-}\mu^+\nu_\mu}$ channels as a function of B^0 decay time. Fit results are overlaid. Relevant for the results is only the slope of the ratios as a function of decay time; absolute ratios, which depend on the decay yields, weighting, and efficiencies, are irrelevant.

of m_{corr} used to measure $\Delta_\Gamma(D)$ but where the ratios of signal and reference yields are determined as functions of the $B_{(s)}^0$ decay time. The decay-time smearing due to the k -factor spread is included in the fit. After the D_s^- lifetime weighting, the decay-time acceptances of simulated signal and reference modes are consistent, with a p value of 83%, and are not included in the fit. The fit is shown in the middle panel of Fig. 3; the resulting width difference is $\Delta_\Gamma(B) = -0.0115 \pm 0.0053 \text{ ps}^{-1}$, with 91% p value.

To check against biases due to differing acceptances and kinematic properties, the analysis is validated with a null test. We repeat the width-difference determination by using the same reference $B^0 \rightarrow [K^+K^-\pi^-]_{D^{(*)-}\mu^+\nu_\mu}$ sample and replacing the signal decays with 2.1×10^6 $B^0 \rightarrow [K^+\pi^-\pi^-]_{D^{(*)-}\mu^+\nu_\mu}$ decays, where the D^- is reconstructed in the $K^+\pi^-\pi^-$ final state (Fig. 3, bottom panel). Differing momentum and vertex-displacement selection criteria induce up to 10% differences between acceptances as a function of D^- decay time and up to 25% variations as a function of B^0 decay time. Acceptance ratios are therefore included in the fit. The p values are 21% for the B^0 fit and 33% for the D^- fit. The resulting width

differences, $\Delta_\Gamma(D) = (-19 \pm 10) \times 10^{-3} \text{ ps}^{-1}$ and $\Delta_\Gamma(B) = (-4.1 \pm 5.4) \times 10^{-3} \text{ ps}^{-1}$, are consistent with zero.

We assess independent systematic uncertainties due to (i) potential fit biases, (ii) assumptions on the components contributing to the sample and their mass distributions, (iii) assumptions on the signal decay model, e.g., choice of $B_s^0 \rightarrow D_s^{*-} \mu^+ \nu_\mu$ form factors, (iv) uncertainties on the decay-time acceptances, (v) uncertainties on the decay-time resolution, (vi) contamination from B_s^0 candidates produced in B_c^+ decays, and (vii) mismodeling of transverse-momentum (p_T) differences between B^0 and B_s^0 mesons. We evaluate each contribution by including the relevant effect in the model and repeating the whole analysis on ensembles of simulated experiments that mirror the data. For the $\Delta_\Gamma(D)$ result, the systematic uncertainty is dominated by a 0.0049 ps^{-1} contribution due to the decay-time acceptance, and a 0.0039 ps^{-1} contribution due to the decay-time resolution. A smaller contribution of 0.0018 ps^{-1} arises from possible mismodeling of p_T differences in B^0 and B_s^0 production. For the $\Delta_\Gamma(B)$ result, a 0.0028 ps^{-1} uncertainty from mismodeling of p_T differences between B^0 and B_s^0 mesons and a 0.0025 ps^{-1} contribution from the B_s^0 decay model dominate. Smaller contributions arise from B_c^+ feed-down (0.0010 ps^{-1}), residual fit biases (0.0009 ps^{-1}), sample composition (0.0005 ps^{-1}), and decay-time acceptance and resolution (0.0004 ps^{-1} each). The uncertainties associated with the limited size of simulated samples are included in the fit χ^2 and contribute up to 20% of the statistical uncertainties. The uncertainty in the decay length has negligible impact. Consistency checks based on repeating the measurement independently on subsamples chosen according to data-taking time, online-selection criteria, charged-particle and vertex multiplicities, momentum of the $K^+ K^- \pi^- \mu^+$ system, and whether only the $D_s^- \mu^+ \nu_\mu$ or the $D_s^{*-} \mu^+ \nu_\mu$ channel is considered as signal, all yield results compatible with statistical fluctuations.

In summary, we report world-leading measurements of B_s^0 and D_s^- meson lifetimes using a novel method. We reconstruct $B_s^0 \rightarrow D_s^{*-} \mu^+ \nu_\mu$ and $B_s^0 \rightarrow D_s^- \mu^+ \nu_\mu$ decays from proton-proton collision data collected by the LHCb experiment and corresponding to 3.0 fb^{-1} of integrated luminosity. We use $B^0 \rightarrow D^{*-} \mu^+ \nu_\mu$ and $B^0 \rightarrow D^- \mu^+ \nu_\mu$ decays reconstructed in the same final state as a reference to suppress systematic uncertainties. The resulting width differences are $\Delta_\Gamma(B) = -0.0115 \pm 0.0053(\text{stat}) \pm 0.0041(\text{syst}) \text{ ps}^{-1}$ and $\Delta_\Gamma(D) = 1.0131 \pm 0.0117(\text{stat}) \pm 0.0065(\text{syst}) \text{ ps}^{-1}$. Their correlation is negligible. Using the known values of the B^0 [8,18] and D^- lifetimes [8,19], we determine the flavor-specific B_s^0 lifetime, $\tau_{B_s^0}^{\text{fs}} = 1.547 \pm 0.013(\text{stat}) \pm 0.010(\text{syst}) \pm 0.004(\tau_B) \text{ ps}$, and the D_s^- lifetime, $\tau_{D_s^-} = 0.5064 \pm 0.0030(\text{stat}) \pm 0.0017(\text{syst}) \pm 0.0017(\tau_D) \text{ ps}$; the last uncertainties are due to the limited knowledge of the

B^0 and D^- lifetime, respectively. The results are consistent with, and significantly more precise than the current values [4–6]. They might offer improved insight into the interplay between strong and weak interactions in the dynamics of heavy mesons and sharpen the reach of current and future indirect searches for nonstandard-model physics.

We thank Alexander Lenz for useful discussions. We express our gratitude to our colleagues in the CERN accelerator departments for the excellent performance of the LHC. We thank the technical and administrative staff at the LHCb institutes. We acknowledge support from CERN and from the national agencies: CAPES, CNPq, FAPERJ and FINEP (Brazil); MOST and NSFC (China); CNRS/IN2P3 (France); BMBF, DFG and MPG (Germany); INFN (Italy); NWO (Netherlands); MNiSW and NCN (Poland); MEN/IFA (Romania); MinES and FASO (Russia); MinECo (Spain); SNSF and SER (Switzerland); NASU (Ukraine); STFC (United Kingdom); NSF (USA). We acknowledge the computing resources that are provided by CERN, IN2P3 (France), KIT and DESY (Germany), INFN (Italy), SURF (Netherlands), PIC (Spain), GridPP (United Kingdom), RRCKI and Yandex LLC (Russia), CSCS (Switzerland), IFIN-HH (Romania), CBPF (Brazil), PL-GRID (Poland) and OSC (USA). We are indebted to the communities behind the multiple open source software packages on which we depend. Individual groups or members have received support from AvH Foundation (Germany), EPLANET, Marie Skłodowska-Curie Actions and ERC (European Union), Conseil Général de Haute-Savoie, Labex ENIGMASS and OCEVU, Région Auvergne (France), RFBR and Yandex LLC (Russia), GVA, XuntaGal and GENCAT (Spain), Herchel Smith Fund, The Royal Society, Royal Commission for the Exhibition of 1851 and the Leverhulme Trust (United Kingdom).

-
- [1] For a recent review, see A. Lenz, Lifetimes and HQE, [arXiv:1405.3601](https://arxiv.org/abs/1405.3601) and references therein.
 - [2] Y. Amhis *et al.* (Heavy Flavor Averaging Group), Averages of b -hadron, c -hadron, and τ -lepton properties as of summer 2016, [arXiv:1612.07233](https://arxiv.org/abs/1612.07233), updated results and plots available at <http://www.slac.stanford.edu/xorg/hfag/>.
 - [3] K. Hartkorn and H. G. Moser, A new method of measuring $\Delta(\Gamma)/\Gamma$ in the $B_s^0 - \bar{B}_s^0$ system, *Eur. Phys. J. C* **8**, 381 (1999).
 - [4] R. Aaij *et al.* (LHCb Collaboration), Measurement of the \bar{B}_s^0 Meson Lifetime in $D_s^+ \pi^-$ Decays, *Phys. Rev. Lett.* **113**, 172001 (2014).
 - [5] V. M. Abazov *et al.* (D0 Collaboration), Measurement of the B_s^0 Lifetime in the Flavor-Specific Decay Channel $B_s^0 \rightarrow D_s^- \mu^+ \nu_X$, *Phys. Rev. Lett.* **114**, 062001 (2015).
 - [6] J. M. Link *et al.* (FOCUS Collaboration), Measurement of the D_s^+ Lifetime, *Phys. Rev. Lett.* **95**, 052003 (2005).
 - [7] K. Kodama *et al.* (Fermilab E653 Collaboration), Measurement of the Relative Branching Fraction

- $\Gamma(D^0 \rightarrow K\mu\nu)/\Gamma(D^0 \rightarrow \mu X)$, *Phys. Rev. Lett.* **66**, 1819 (1991).
- [8] C. Patrignani *et al.* (Particle Data Group), Review of particle physics, *Chin. Phys. C* **40**, 100001 (2016).
- [9] A. Abulencia *et al.* (CDF Collaboration), Observation of $B_s^0 - \bar{B}_s^0$ Oscillations, *Phys. Rev. Lett.* **97**, 242003 (2006).
- [10] N. T. Leonardo, Ph.D. thesis, FERMI-LAB-THESIS-2006-18, 2006.
- [11] A. A. Alves Jr. *et al.* (LHCb Collaboration), The LHCb detector at the LHC, *J. Instrum.* **3**, S08005 (2008).
- [12] R. Aaij *et al.* (LHCb Collaboration), LHCb detector performance, *Int. J. Mod. Phys. A* **30**, 1530022 (2015).
- [13] M. Clemencic, G. Corti, S. Easo, C. R. Jones, S. Miglioranza, M. Pappagallo, and P. Robbe, The LHCb simulation application, Gauss: Design, evolution and experience, *J. Phys. Conf. Ser.* **331**, 032023 (2011).
- [14] I. Belyaev *et al.*, Handling of the generation of primary events in Gauss, the LHCb simulation framework, *J. Phys. Conf. Ser.* **331**, 032047 (2011).
- [15] I. Caprini, L. Lellouch, and M. Neubert, Dispersive bounds on the shape of $B^0 \rightarrow D^{(*)}\ell\bar{\nu}_\ell$ form factors, *Nucl. Phys.* **B530**, 153 (1998).
- [16] R. Aaij *et al.*, The LHCb trigger and its performance in 2011, *J. Instrum.* **8**, P04022 (2013).
- [17] The symbol $D_{(s)}^{**}$ identifies collectively higher orbital excitations of $D_{(s)}^-$ mesons.
- [18] R. Aaij *et al.* (LHCb Collaboration), Measurements of the B^+ , B^0 , B_s^0 meson and Λ_b^0 baryon lifetimes, *J. High Energy Phys.* **04** (2014) 114.
- [19] J. M. Link *et al.* (FOCUS Collaboration), New measurements of the D^0 and D^+ lifetimes, *Phys. Lett. B* **537**, 192 (2002).

R. Aaij,⁴⁰ B. Adeva,³⁹ M. Adinolfi,⁴⁸ Z. Ajaltouni,⁵ S. Akar,⁵⁹ J. Albrecht,¹⁰ F. Alessio,⁴⁰ M. Alexander,⁵³ S. Ali,⁴³ G. Alkhazov,³¹ P. Alvarez Cartelle,⁵⁵ A. A. Alves Jr.,⁵⁹ S. Amato,² S. Amerio,²³ Y. Amhis,⁷ L. An,³ L. Anderlini,¹⁸ G. Andreassi,⁴¹ M. Andreotti,^{17,a} J. E. Andrews,⁶⁰ R. B. Appleby,⁵⁶ F. Archilli,⁴³ P. d'Argent,¹² J. Arnau Romeu,⁶ A. Artamonov,³⁷ M. Artuso,⁶¹ E. Aslanides,⁶ G. Aurieremma,²⁶ M. Baalouch,⁵ I. Babuschkin,⁵⁶ S. Bachmann,¹² J. J. Back,⁵⁰ A. Badalov,³⁸ C. Baesso,⁶² S. Baker,⁵⁵ V. Balagura,^{7,b} W. Baldini,¹⁷ A. Baranov,³⁵ R. J. Barlow,⁵⁶ C. Barschel,⁴⁰ S. Barsuk,⁷ W. Barter,⁵⁶ F. Baryshnikov,³² M. Baszczyk,²⁷ V. Batozskaya,²⁹ B. Batsukh,⁶¹ V. Battista,⁴¹ A. Bay,⁴¹ L. Beaucourt,⁴ J. Beddow,⁵³ F. Bedeschi,²⁴ I. Bediaga,¹ A. Beiter,⁶¹ L. J. Bel,⁴³ V. Bellee,⁴¹ N. Belloli,^{21,c} K. Belous,³⁷ I. Belyaev,³² E. Ben-Haim,⁸ G. Bencivenni,¹⁹ S. Benson,⁴³ S. Beranek,⁹ A. Berezhnoy,³³ R. Bernet,⁴² A. Bertolin,²³ C. Betancourt,⁴² F. Betti,¹⁵ M.-O. Bettler,⁴⁰ M. van Beuzekom,⁴³ I. A. Bezshyko,⁴² S. Bifani,⁴⁷ P. Billoir,⁸ A. Birnkraut,¹⁰ A. Bitadze,⁵⁶ A. Bizzeti,^{18,d} T. Blake,⁵⁰ F. Blanc,⁴¹ J. Blouw,¹¹ S. Blusk,⁶¹ V. Bocci,²⁶ T. Boettcher,⁵⁸ A. Bondar,^{36,e} N. Bondar,³¹ W. Bonivento,¹⁶ I. Bordyuzhin,³² A. Borgheresi,^{21,c} S. Borghi,⁵⁶ M. Borisyak,³⁵ M. Borsato,³⁹ F. Bossu,⁷ M. Boubdir,⁹ T. J. V. Bowcock,⁵⁴ E. Bowen,⁴² C. Bozzi,^{17,40} S. Braun,¹² T. Britton,⁶¹ J. Brodzicka,⁵⁶ E. Buchanan,⁴⁸ C. Burr,⁵⁶ A. Bursche,² J. Buytaert,⁴⁰ S. Cadeddu,¹⁶ R. Calabrese,^{17,a} M. Calvi,^{21,c} M. Calvo Gomez,^{38,f} A. Camboni,³⁸ P. Campana,¹⁹ D. H. Campora Perez,⁴⁰ L. Capriotti,⁵⁶ A. Carbone,^{15,g} G. Carboni,^{25,h} R. Cardinale,^{20,i} A. Cardini,¹⁶ P. Carniti,^{21,c} L. Carson,⁵² K. Carvalho Akiba,² G. Casse,⁵⁴ L. Cassina,^{21,c} L. Castillo Garcia,⁴¹ M. Cattaneo,⁴⁰ G. Cavallero,²⁰ R. Cenci,^{24,j} D. Chamont,⁷ M. Charles,⁸ Ph. Charpentier,⁴⁰ G. Chatzikonstantinidis,⁴⁷ M. Chefdeville,⁴ S. Chen,⁵⁶ S.-F. Cheung,⁵⁷ V. Chobanova,³⁹ M. Chrzaszcz,^{42,27} A. Chubykin,³¹ X. Cid Vidal,³⁹ G. Ciezarek,⁴³ P. E. L. Clarke,⁵² M. Clemencic,⁴⁰ H. V. Cliff,⁴⁹ J. Closier,⁴⁰ V. Coco,⁵⁹ J. Cogan,⁶ E. Cogneras,⁵ V. Cogoni,^{16,k} L. Cojocariu,³⁰ P. Collins,⁴⁰ A. Comerma-Montells,¹² A. Contu,⁴⁰ A. Cook,⁴⁸ G. Coombs,⁴⁰ S. Coquereau,³⁸ G. Corti,⁴⁰ M. Corvo,^{17,a} C. M. Costa Sobral,⁵⁰ B. Couturier,⁴⁰ G. A. Cowan,⁵² D. C. Craik,⁵² A. Crocombe,⁵⁰ M. Cruz Torres,⁶² S. Cunliffe,⁵⁵ R. Currie,⁵² C. D'Ambrosio,⁴⁰ F. Da Cunha Marinho,² E. Dall'Occo,⁴³ J. Dalseno,⁴⁸ P. N. Y. David,⁴³ A. Davis,³ K. De Bruyn,⁶ S. De Capua,⁵⁶ M. De Cian,¹² J. M. De Miranda,¹ L. De Paula,² M. De Serio,^{14,l} P. De Simone,¹⁹ C. T. Dean,⁵³ D. Decamp,⁴ M. Deckenhoff,¹⁰ L. Del Buono,⁸ H.-P. Dembinski,¹¹ M. Demmer,¹⁰ A. Dendek,²⁸ D. Derkach,³⁵ O. Deschamps,⁵ F. Dettori,⁵⁴ B. Dey,²² A. Di Canto,⁴⁰ P. Di Nezza,¹⁹ H. Dijkstra,⁴⁰ F. Dordei,⁴⁰ M. Dorigo,⁴¹ A. Dosil Suárez,³⁹ A. Dovbnya,⁴⁵ K. Dreimanis,⁵⁴ L. Dufour,⁴³ G. Dujany,⁵⁶ K. Dungs,⁴⁰ P. Durante,⁴⁰ R. Dzhelezadine,³⁷ M. Dziewiecki,¹² A. Dziurda,⁴⁰ A. Dzyuba,³¹ N. Déléage,⁴ S. Easo,⁵¹ M. Ebert,⁵² U. Egede,⁵⁵ V. Egorychev,³² S. Eidelman,^{36,e} S. Eisenhardt,⁵² U. Eitschberger,¹⁰ R. Ekelhof,¹⁰ L. Eklund,⁵³ S. Ely,⁶¹ S. Esen,¹² H. M. Evans,⁴⁹ T. Evans,⁵⁷ A. Falabella,¹⁵ N. Farley,⁴⁷ S. Farry,⁵⁴ R. Fay,⁵⁴ D. Fazzini,^{21,c} D. Ferguson,⁵² G. Fernandez,³⁸ A. Fernandez Prieto,³⁹ F. Ferrari,¹⁵ F. Ferreira Rodrigues,² M. Ferro-Luzzi,⁴⁰ S. Filippov,³⁴ R. A. Fini,¹⁴ M. Fiore,^{17,a} M. Fiorini,^{17,a} M. Firlej,²⁸ C. Fitzpatrick,⁴¹ T. Fiutowski,²⁸ F. Fleuret,^{7,m} K. Fohl,⁴⁰ M. Fontana,^{16,40} F. Fontanelli,^{20,i} D. C. Forshaw,⁶¹ R. Forty,⁴⁰ V. Franco Lima,⁵⁴ M. Frank,⁴⁰ C. Frei,⁴⁰ J. Fu,^{22,n} W. Funk,⁴⁰ E. Furfaro,^{25,h} C. Färber,⁴⁰ A. Gallas Torreira,³⁹ D. Galli,^{15,g} S. Gallorini,²³ S. Gambetta,⁵² M. Gandelman,² P. Gandini,⁵⁷ Y. Gao,³ L. M. Garcia Martin,⁶⁹ J. García Pardiñas,³⁹

J. Garra Tico,⁴⁹ L. Garrido,³⁸ P. J. Garsed,⁴⁹ D. Gascon,³⁸ C. Gaspar,⁴⁰ L. Gavardi,¹⁰ G. Gazzoni,⁵ D. Gerick,¹² E. Gersabeck,¹² M. Gersabeck,⁵⁶ T. Gershon,⁵⁰ Ph. Ghez,⁴ S. Gianì,⁴¹ V. Gibson,⁴⁹ O. G. Girard,⁴¹ L. Giubega,³⁰ K. Gizdov,⁵² V. V. Gligorov,⁸ D. Golubkov,³² A. Golutvin,^{55,40} A. Gomes,^{1,0} I. V. Gorelov,³³ C. Gotti,^{21,c} E. Govorkova,⁴³ R. Graciani Diaz,³⁸ L. A. Granado Cardoso,⁴⁰ E. Graugés,³⁸ E. Graverini,⁴² G. Graziani,¹⁸ A. Grecu,³⁰ R. Greim,⁹ P. Griffith,¹⁶ L. Grillo,^{21,40,c} B. R. Gruberg Cazon,⁵⁷ O. Grünberg,⁶⁷ E. Gushchin,³⁴ Yu. Guz,³⁷ T. Gys,⁴⁰ C. Göbel,⁶² T. Hadavizadeh,⁵⁷ C. Hadjivasiliou,⁵ G. Haefeli,⁴¹ C. Haen,⁴⁰ S. C. Haines,⁴⁹ B. Hamilton,⁶⁰ X. Han,¹² S. Hansmann-Menzemer,¹² N. Harnew,⁵⁷ S. T. Harnew,⁴⁸ J. Harrison,⁵⁶ M. Hatch,⁴⁰ J. He,⁶³ T. Head,⁴¹ A. Heister,⁹ K. Hennessy,⁵⁴ P. Henrard,⁵ L. Henry,⁶⁹ E. van Herwijnen,⁴⁰ M. Heß,⁶⁷ A. Hicheur,² D. Hill,⁵⁷ C. Hombach,⁵⁶ H. Hopchev,⁴¹ Z.-C. Huard,⁵⁹ W. Hulsbergen,⁴³ T. Humair,⁵⁵ M. Hushchyn,³⁵ D. Hutchcroft,⁵⁴ M. Idzik,²⁸ P. Ilten,⁵⁸ R. Jacobsson,⁴⁰ J. Jalocha,⁵⁷ E. Jans,⁴³ A. Jawahery,⁶⁰ F. Jiang,³ M. John,⁵⁷ D. Johnson,⁴⁰ C. R. Jones,⁴⁹ C. Joram,⁴⁰ B. Jost,⁴⁰ N. Jurik,⁵⁷ S. Kandybei,⁴⁵ M. Karacson,⁴⁰ J. M. Kariuki,⁴⁸ S. Karodia,⁵³ M. Kecke,¹² M. Kelsey,⁶¹ M. Kenzie,⁴⁹ T. Ketel,⁴⁴ E. Khairullin,³⁵ B. Khanji,¹² C. Khurewathanakul,⁴¹ T. Kim,⁹ S. Klaver,⁵⁶ K. Klimaszewski,²⁹ T. Klimkovich,¹¹ S. Koliiev,⁴⁶ M. Kolpin,¹² I. Komarov,⁴¹ R. Kopečna,¹² P. Koppenburg,⁴³ A. Kosmyntseva,³² S. Kotriakhova,³¹ A. Kozachuk,³³ M. Kozeiha,⁵ L. Kravchuk,³⁴ M. Kreps,⁵⁰ P. Krokovny,^{36,e} F. Kruse,¹⁰ W. Krzemien,²⁹ W. Kucewicz,^{27,p} M. Kucharczyk,²⁷ V. Kudryavtsev,^{36,e} A. K. Kuonen,⁴¹ K. Kurek,²⁹ T. Kvaratskheliya,^{32,40} D. Lacarrere,⁴⁰ G. Lafferty,⁵⁶ A. Lai,¹⁶ G. Lanfranchi,¹⁹ C. Langenbruch,⁹ T. Latham,⁵⁰ C. Lazzeroni,⁴⁷ R. Le Gac,⁶ J. van Leerdam,⁴³ A. Leflat,^{33,40} J. Lefrançois,⁷ R. Lefèvre,⁵ F. Lemaitre,⁴⁰ E. Lemos Cid,³⁹ O. Leroy,⁶ T. Lesiak,²⁷ B. Leverington,¹² T. Li,³ Y. Li,⁷ Z. Li,⁶¹ T. Likhomanenko,^{35,68} R. Lindner,⁴⁰ F. Lionetto,⁴² X. Liu,³ D. Loh,⁵⁰ I. Longstaff,⁵³ J. H. Lopes,² D. Lucchesi,^{23,q} M. Lucio Martinez,³⁹ H. Luo,⁵² A. Lupato,²³ E. Luppi,^{17,a} O. Lupton,⁴⁰ A. Lusiani,²⁴ X. Lyu,⁶³ F. Machefert,⁷ F. Maciuc,³⁰ O. Maev,³¹ K. Maguire,⁵⁶ S. Malde,⁵⁷ A. Malinin,⁶⁸ T. Maltsev,³⁶ G. Manca,^{16,k} G. Mancinelli,⁶ P. Manning,⁶¹ J. Maratas,^{5,r} J. F. Marchand,⁴ U. Marconi,¹⁵ C. Marin Benito,³⁸ M. Marinangeli,⁴¹ P. Marino,^{24,j} J. Marks,¹² G. Martellotti,²⁶ M. Martin,⁶ M. Martinelli,⁴¹ D. Martinez Santos,³⁹ F. Martinez Vidal,⁶⁹ D. Martins Tostes,² L. M. Massacrier,⁷ A. Massafferri,¹ R. Matev,⁴⁰ A. Mathad,⁵⁰ Z. Mathe,⁴⁰ C. Matteuzzi,²¹ A. Mauri,⁴² E. Maurice,^{7,m} B. Maurin,⁴¹ A. Mazurov,⁴⁷ M. McCann,^{55,40} A. McNab,⁵⁶ R. McNulty,¹³ B. Meadows,⁵⁹ F. Meier,¹⁰ D. Melnychuk,²⁹ M. Merk,⁴³ A. Merli,^{22,n} E. Michielin,²³ D. A. Milanes,⁶⁶ M.-N. Minard,⁴ D. S. Mitzel,¹² A. Mogini,⁸ J. Molina Rodriguez,¹ I. A. Monroy,⁶⁶ S. Monteil,⁵ M. Morandin,²³ M. J. Morello,^{24,j} O. Morgunova,⁶⁸ J. Moron,²⁸ A. B. Morris,⁵² R. Mountain,⁶¹ F. Muheim,⁵² M. Mulder,⁴³ M. Mussini,¹⁵ D. Müller,⁵⁶ J. Müller,¹⁰ K. Müller,⁴² V. Müller,¹⁰ P. Naik,⁴⁸ T. Nakada,⁴¹ R. Nandakumar,⁵¹ A. Nandi,⁵⁷ I. Nasteva,² M. Needham,⁵² N. Neri,^{22,40} S. Neubert,¹² N. Neufeld,⁴⁰ M. Neuner,¹² T. D. Nguyen,⁴¹ C. Nguyen-Mau,^{41,s} S. Nieswand,⁹ R. Niet,¹⁰ N. Nikitin,³³ T. Nikodem,¹² A. Nogay,⁶⁸ A. Novoselov,³⁷ D. P. O'Hanlon,⁵⁰ A. Oblakowska-Mucha,²⁸ V. Obraztsov,³⁷ S. Ogilvy,¹⁹ R. Oldeman,^{16,k} C. J. G. Onderwater,⁷⁰ A. Ossowska,²⁷ J. M. Otalora Goicochea,² P. Owen,⁴² A. Oyanguren,⁶⁹ P. R. Pais,⁴¹ A. Palano,^{14,1} M. Palutan,^{19,40} A. Papanestis,⁵¹ M. Pappagallo,^{14,1} L. L. Pappalardo,^{17,a} C. Pappenheimer,⁵⁹ W. Parker,⁶⁰ C. Parkes,⁵⁶ G. Passaleva,¹⁸ A. Pastore,^{14,1} M. Patel,⁵⁵ C. Patrignani,^{15,g} A. Pearce,⁴⁰ A. Pellegrino,⁴³ G. Penso,²⁶ M. Pepe Altarelli,⁴⁰ S. Perazzini,⁴⁰ P. Perret,⁵ L. Pescatore,⁴¹ K. Petridis,⁴⁸ A. Petrolini,^{20,i} A. Petrov,⁶⁸ M. Petruzzo,^{22,n} E. Picatoste Olloqui,³⁸ B. Pietrzyk,⁴ M. Pikiés,²⁷ D. Pinci,²⁶ A. Pistone,²⁰ A. Piucci,¹² V. Placinta,³⁰ S. Playfer,⁵² M. Plo Casasus,³⁹ T. Poikela,⁴⁰ F. Polci,⁸ M. Poli Lener,¹⁹ A. Poluektov,^{50,36} I. Polyakov,⁶¹ E. Polycarpo,² G. J. Pomery,⁴⁸ S. Ponce,⁴⁰ A. Popov,³⁷ D. Popov,^{11,40} B. Popovici,³⁰ S. Poslavskii,³⁷ C. Potterat,² E. Price,⁴⁸ J. Prisciandaro,³⁹ C. Prouve,⁴⁸ V. Pugatch,⁴⁶ A. Puig Navarro,⁴² G. Punzi,^{24,t} C. Qian,⁶³ W. Qian,⁵⁰ R. Quagliani,^{7,48} B. Rachwal,²⁸ J. H. Rademacker,⁴⁸ M. Rama,²⁴ M. Ramos Pernas,³⁹ M. S. Rangel,² I. Raniuk,⁴⁵ F. Ratnikov,³⁵ G. Raven,⁴⁴ F. Redi,⁵⁵ S. Reichert,¹⁰ A. C. dos Reis,¹ C. Remon Alepuz,⁶⁹ V. Renaudin,⁷ S. Ricciardi,⁵¹ S. Richards,⁴⁸ M. Rihl,⁴⁰ K. Rinnert,⁵⁴ V. Rives Molina,³⁸ P. Robbe,⁷ A. B. Rodrigues,¹ E. Rodrigues,⁵⁹ J. A. Rodriguez Lopez,⁶⁶ P. Rodriguez Perez,⁵⁶ A. Rogozhnikov,³⁵ S. Roiser,⁴⁰ A. Rollings,⁵⁷ V. Romanovskiy,³⁷ A. Romero Vidal,³⁹ J. W. Ronayne,¹³ M. Rotondo,¹⁹ M. S. Rudolph,⁶¹ T. Ruf,⁴⁰ P. Ruiz Valls,⁶⁹ J. J. Saborido Silva,³⁹ E. Sadykhov,³² N. Sagidova,³¹ B. Saitta,^{16,k} V. Salustino Guimaraes,¹ D. Sanchez Gonzalo,³⁸ C. Sanchez Mayordomo,⁶⁹ B. Sanmartin Sedes,³⁹ R. Santacesaria,²⁶ C. Santamarina Rios,³⁹ M. Santimaria,¹⁹ E. Santovetti,^{25,h} A. Sarti,^{19,u} C. Satriano,^{26,v} A. Satta,²⁵ D. M. Saunders,⁴⁸ D. Savrina,^{32,33} S. Schael,⁹ M. Schellenberg,¹⁰ M. Schiller,⁵³ H. Schindler,⁴⁰ M. Schlupp,¹⁰ M. Schmelling,¹¹ T. Schmelzer,¹⁰ B. Schmidt,⁴⁰ O. Schneider,⁴¹ A. Schopper,⁴⁰ H. F. Schreiner,⁵⁹ K. Schubert,¹⁰ M. Schubiger,⁴¹ M.-H. Schune,⁷ R. Schwemmer,⁴⁰ B. Sciascia,¹⁹ A. Sciubba,^{26,u} A. Semennikov,³² A. Sergi,⁴⁷ N. Serra,⁴² J. Serrano,⁶ L. Sestini,²³ P. Seyfert,²¹ M. Shapkin,³⁷ I. Shapoval,⁴⁵ Y. Shcheglov,³¹ T. Shears,⁵⁴ L. Shekhtman,^{36,e} V. Shevchenko,⁶⁸ B. G. Siddi,^{17,40} R. Silva Coutinho,⁴² L. Silva de Oliveira,² G. Simi,^{23,q} S. Simone,^{14,1}

M. Sirendi,⁴⁹ N. Skidmore,⁴⁸ T. Skwarnicki,⁶¹ E. Smith,⁵⁵ I. T. Smith,⁵² J. Smith,⁴⁹ M. Smith,⁵⁵ I. Soares Lavra,¹ M. D. Sokoloff,⁵⁹ F. J. P. Soler,⁵³ B. Souza De Paula,² B. Spaan,¹⁰ P. Spradlin,⁵³ S. Sridharan,⁴⁰ F. Stagni,⁴⁰ M. Stahl,¹² S. Stahl,⁴⁰ P. Stefko,⁴¹ S. Stefkova,⁵⁵ O. Steinkamp,⁴² S. Stemmler,¹² O. Stenyakin,³⁷ H. Stevens,¹⁰ S. Stoica,³⁰ S. Stone,⁶¹ B. Storaci,⁴² S. Stracka,^{24,t} M. E. Stramaglia,⁴¹ M. Straticiu,³⁰ U. Straumann,⁴² L. Sun,⁶⁴ W. Sutcliffe,⁵⁵ K. Swientek,²⁸ V. Syropoulos,⁴⁴ M. Szczekowski,²⁹ T. Szumlak,²⁸ S. T’Jampens,⁴ A. Tayduganov,⁶ T. Tekampe,¹⁰ G. Tellarini,^{17,a} F. Teubert,⁴⁰ E. Thomas,⁴⁰ J. van Tilburg,⁴³ M. J. Tilley,⁵⁵ V. Tisserand,⁴ M. Tobin,⁴¹ S. Tolk,⁴⁹ L. Tomassetti,^{17,a} D. Tonelli,²⁴ S. Topp-Joergensen,⁵⁷ F. Toriello,⁶¹ R. Tourinho Jadallah Aoude,¹ E. Tournefier,⁴ S. Tourneur,⁴¹ K. Trabelsi,⁴¹ M. Traill,⁵³ M. T. Tran,⁴¹ M. Tresch,⁴² A. Trisovic,⁴⁰ A. Tsaregorodtsev,⁶ P. Tsopelas,⁴³ A. Tully,⁴⁹ N. Tuning,⁴³ A. Ukleja,²⁹ A. Ustyuzhanin,³⁵ U. Uwer,¹² C. Vacca,^{16,k} V. Vagnoni,^{15,40} A. Valassi,⁴⁰ S. Valat,⁴⁰ G. Valenti,¹⁵ R. Vazquez Gomez,¹⁹ P. Vazquez Regueiro,³⁹ S. Vecchi,¹⁷ M. van Veghel,⁴³ J. J. Velthuis,⁴⁸ M. Veltri,^{18,w} G. Veneziano,⁵⁷ A. Venkateswaran,⁶¹ T. A. Verlage,⁹ M. Vernet,⁵ M. Vesterinen,¹² J. V. Viana Barbosa,⁴⁰ B. Viaud,⁷ D. Vieira,⁶³ M. Vieites Diaz,³⁹ H. Viemann,⁶⁷ X. Vilasis-Cardona,^{38,f} M. Vitti,⁴⁹ V. Volkov,³³ A. Vollhardt,⁴² B. Voneki,⁴⁰ A. Vorobyev,³¹ V. Vorobyev,^{36,e} C. Voß,⁹ J. A. de Vries,⁴³ C. Vázquez Sierra,³⁹ R. Waldi,⁶⁷ C. Wallace,⁵⁰ R. Wallace,¹³ J. Walsh,²⁴ J. Wang,⁶¹ D. R. Ward,⁴⁹ H. M. Wark,⁵⁴ N. K. Watson,⁴⁷ D. Websdale,⁵⁵ A. Weiden,⁴² M. Whitehead,⁴⁰ J. Wicht,⁵⁰ G. Wilkinson,^{57,40} M. Wilkinson,⁶¹ M. Williams,⁴⁰ M. P. Williams,⁴⁷ M. Williams,⁵⁸ T. Williams,⁴⁷ F. F. Wilson,⁵¹ J. Wimberley,⁶⁰ M. A. Winn,⁷ J. Wishahi,¹⁰ W. Wislicki,²⁹ M. Witek,²⁷ G. Wormser,⁷ S. A. Wotton,⁴⁹ K. Wraight,⁵³ K. Wyllie,⁴⁰ Y. Xie,⁶⁵ Z. Xing,⁶¹ Z. Xu,⁴ Z. Yang,³ Z. Yang,⁶⁰ Y. Yao,⁶¹ H. Yin,⁶⁵ J. Yu,⁶⁵ X. Yuan,^{36,e} O. Yushchenko,³⁷ K. A. Zarebski,⁴⁷ M. Zavertyaev,^{11,b} L. Zhang,³ Y. Zhang,⁷ A. Zhelezov,¹² Y. Zheng,⁶³ X. Zhu,³ V. Zhukov,³³ and S. Zucchelli¹⁵

(LHCb Collaboration)

¹Centro Brasileiro de Pesquisas Físicas (CBPF), Rio de Janeiro, Brazil²Universidade Federal do Rio de Janeiro (UFRJ), Rio de Janeiro, Brazil³Center for High Energy Physics, Tsinghua University, Beijing, China⁴LAPP, Université Savoie Mont-Blanc, CNRS/IN2P3, Annecy-Le-Vieux, France⁵Clermont Université, Université Blaise Pascal, CNRS/IN2P3, LPC, Clermont-Ferrand, France⁶CPPM, Aix-Marseille Université, CNRS/IN2P3, Marseille, France⁷LAL, Université Paris-Sud, CNRS/IN2P3, Orsay, France⁸LPNHE, Université Pierre et Marie Curie, Université Paris Diderot, CNRS/IN2P3, Paris, France⁹I. Physikalisches Institut, RWTH Aachen University, Aachen, Germany¹⁰Fakultät Physik, Technische Universität Dortmund, Dortmund, Germany¹¹Max-Planck-Institut für Kernphysik (MPIK), Heidelberg, Germany¹²Physikalisches Institut, Ruprecht-Karls-Universität Heidelberg, Heidelberg, Germany¹³School of Physics, University College Dublin, Dublin, Ireland¹⁴Sezione INFN di Bari, Bari, Italy¹⁵Sezione INFN di Bologna, Bologna, Italy¹⁶Sezione INFN di Cagliari, Cagliari, Italy¹⁷Sezione INFN di Ferrara, Ferrara, Italy¹⁸Sezione INFN di Firenze, Firenze, Italy¹⁹Laboratori Nazionali dell’INFN di Frascati, Frascati, Italy²⁰Sezione INFN di Genova, Genova, Italy²¹Sezione INFN di Milano Bicocca, Milano, Italy²²Sezione INFN di Milano, Milano, Italy²³Sezione INFN di Padova, Padova, Italy²⁴Sezione INFN di Pisa, Pisa, Italy²⁵Sezione INFN di Roma Tor Vergata, Roma, Italy²⁶Sezione INFN di Roma La Sapienza, Roma, Italy²⁷Henryk Niewodniczanski Institute of Nuclear Physics Polish Academy of Sciences, Kraków, Poland²⁸AGH - University of Science and Technology, Faculty of Physics and Applied Computer Science, Kraków, Poland²⁹National Center for Nuclear Research (NCBJ), Warsaw, Poland³⁰Horia Hulubei National Institute of Physics and Nuclear Engineering, Bucharest-Magurele, Romania³¹Petersburg Nuclear Physics Institute (PNPI), Gatchina, Russia³²Institute of Theoretical and Experimental Physics (ITEP), Moscow, Russia³³Institute of Nuclear Physics, Moscow State University (SINP MSU), Moscow, Russia

- ³⁴*Institute for Nuclear Research of the Russian Academy of Sciences (INR RAN), Moscow, Russia*
- ³⁵*Yandex School of Data Analysis, Moscow, Russia*
- ³⁶*Budker Institute of Nuclear Physics (SB RAS), Novosibirsk, Russia*
- ³⁷*Institute for High Energy Physics (IHEP), Protvino, Russia*
- ³⁸*ICCUB, Universitat de Barcelona, Barcelona, Spain*
- ³⁹*Universidad de Santiago de Compostela, Santiago de Compostela, Spain*
- ⁴⁰*European Organization for Nuclear Research (CERN), Geneva, Switzerland*
- ⁴¹*Institute of Physics, Ecole Polytechnique Fédérale de Lausanne (EPFL), Lausanne, Switzerland*
- ⁴²*Physik-Institut, Universität Zürich, Zürich, Switzerland*
- ⁴³*Nikhef National Institute for Subatomic Physics, Amsterdam, Netherlands*
- ⁴⁴*Nikhef National Institute for Subatomic Physics and VU University Amsterdam, Amsterdam, Netherlands*
- ⁴⁵*NSC Kharkiv Institute of Physics and Technology (NSC KIPT), Kharkiv, Ukraine*
- ⁴⁶*Institute for Nuclear Research of the National Academy of Sciences (KINR), Kyiv, Ukraine*
- ⁴⁷*University of Birmingham, Birmingham, United Kingdom*
- ⁴⁸*H.H. Wills Physics Laboratory, University of Bristol, Bristol, United Kingdom*
- ⁴⁹*Cavendish Laboratory, University of Cambridge, Cambridge, United Kingdom*
- ⁵⁰*Department of Physics, University of Warwick, Coventry, United Kingdom*
- ⁵¹*STFC Rutherford Appleton Laboratory, Didcot, United Kingdom*
- ⁵²*School of Physics and Astronomy, University of Edinburgh, Edinburgh, United Kingdom*
- ⁵³*School of Physics and Astronomy, University of Glasgow, Glasgow, United Kingdom*
- ⁵⁴*Oliver Lodge Laboratory, University of Liverpool, Liverpool, United Kingdom*
- ⁵⁵*Imperial College London, London, United Kingdom*
- ⁵⁶*School of Physics and Astronomy, University of Manchester, Manchester, United Kingdom*
- ⁵⁷*Department of Physics, University of Oxford, Oxford, United Kingdom*
- ⁵⁸*Massachusetts Institute of Technology, Cambridge, Massachusetts, USA*
- ⁵⁹*University of Cincinnati, Cincinnati, Ohio, USA*
- ⁶⁰*University of Maryland, College Park, Maryland, USA*
- ⁶¹*Syracuse University, Syracuse, New York, USA*
- ⁶²*Pontifícia Universidade Católica do Rio de Janeiro (PUC-Rio), Rio de Janeiro, Brazil*
(associated with *Institution Universidade Federal do Rio de Janeiro (UFRJ), Rio de Janeiro, Brazil*)
- ⁶³*University of Chinese Academy of Sciences, Beijing, China*
(associated with *Institution Center for High Energy Physics, Tsinghua University, Beijing, China*)
- ⁶⁴*School of Physics and Technology, Wuhan University, Wuhan, China*
(associated with *Institution Center for High Energy Physics, Tsinghua University, Beijing, China*)
- ⁶⁵*Institute of Particle Physics, Central China Normal University, Wuhan, Hubei, China*
(associated with *Institution Center for High Energy Physics, Tsinghua University, Beijing, China*)
- ⁶⁶*Departamento de Física, Universidad Nacional de Colombia, Bogota, Colombia*
(associated with *Institution LPNHE, Université Pierre et Marie Curie, Université Paris Diderot, CNRS/IN2P3, Paris, France*)
- ⁶⁷*Institut für Physik, Universität Rostock, Rostock, Germany*
(associated with *Institution Physikalisches Institut, Ruprecht-Karls-Universität Heidelberg, Heidelberg, Germany*)
- ⁶⁸*National Research Centre Kurchatov Institute, Moscow, Russia*
(associated with *Institution Institute of Theoretical and Experimental Physics (ITEP), Moscow, Russia*)
- ⁶⁹*Instituto de Física Corpuscular, Centro Mixto Universidad de Valencia - CSIC, Valencia, Spain*
(associated with *Institution ICCUB, Universitat de Barcelona, Barcelona, Spain*)
- ⁷⁰*Van Swinderen Institute, University of Groningen, Groningen, Netherlands*
(associated with *Institution Nikhef National Institute for Subatomic Physics, Amsterdam, Netherlands*)

^aAlso at Università di Ferrara, Ferrara, Italy.

^bAlso at P.N. Lebedev Physical Institute, Russian Academy of Science (LPI RAS), Moscow, Russia.

^cAlso at Università di Milano Bicocca, Milano, Italy.

^dAlso at Università di Modena e Reggio Emilia, Modena, Italy.

^eAlso at Novosibirsk State University, Novosibirsk, Russia.

^fAlso at LIFAELS, La Salle, Universitat Ramon Llull, Barcelona, Spain.

^gAlso at Università di Bologna, Bologna, Italy.

^hAlso at Università di Roma Tor Vergata, Roma, Italy.

ⁱAlso at Università di Genova, Genova, Italy.

^jAlso at Scuola Normale Superiore, Pisa, Italy.

^kAlso at Università di Cagliari, Cagliari, Italy.

^lAlso at Università di Bari, Bari, Italy.

^mAlso at Laboratoire Leprince-Ringuet, Palaiseau, France.

ⁿAlso at Università degli Studi di Milano, Milano, Italy.

^oAlso at Universidade Federal do Triângulo Mineiro (UFTM), Uberaba-MG, Brazil.

^pAlso at AGH - University of Science and Technology, Faculty of Computer Science, Electronics and Telecommunications, Kraków, Poland.

^qAlso at Università di Padova, Padova, Italy.

^rAlso at Iligan Institute of Technology (IIT), Iligan, Philippines.

^sAlso at Hanoi University of Science, Hanoi, Vietnam.

^tAlso at Università di Pisa, Pisa, Italy.

^uAlso at Università di Roma La Sapienza, Roma, Italy.

^vAlso at Università della Basilicata, Potenza, Italy.

^wAlso at Università di Urbino, Urbino, Italy.